Biosensors and Bioelectronics 41 (2013) 316–321

Contents lists available at SciVerse ScienceDirect

Biosensors and Bioelectronics

journal homepage: www.elsevier.com/locate/bios

Surface-enhanced Raman scattering (SERS) detection of multiple viral antigens using magnetic capture of SERS-active nanoparticles

Jing Neng [a,b], Mark H. Harpster [b], William C. Wilson [c], Patrick A. Johnson [a,b,*]

[a] Molecular and Cellular Life Sciences Program, University of Wyoming, Laramie, WY 82071, United States
[b] Department of Chemical and Petroleum Engineering, University of Wyoming, Laramie, WY 82071, United States
[c] Arthropod-Borne Animal Diseases Research Unit, Center for Grain and Animal Health Research, USDA/ARS, Manhattan, KS 66502, United States

ARTICLE INFO

Article history:
Received 11 June 2012
Received in revised form
14 August 2012
Accepted 21 August 2012
Available online 29 August 2012

Keywords:
SERS
Immunoassay
Multiplex
Gold nanoparticle
Paramagnetic nanoparticle

ABSTRACT

A highly sensitive immunoassay based on surface-enhanced Raman scattering (SERS) spectroscopy has been developed for multiplex detection of surface envelope and capsid antigens of the viral zoonotic pathogens West Nile virus (WNV) and Rift Valley fever virus (RVFV). Detection was mediated by antibody recognition using Raman reporter-coated Au nanoparticles (GNPs) and paramagnetic nanoparticles (PMPs) conjugated with polyclonal antibodies specific for each antigen target, followed by 785 nm laser excitation of magnetically concentrated GNP/antigen/PMP complexes. The discrimination of WNV and RVFV antigen detection in mixed Raman spectra was achieved by SERS enhancement of Raman spectra specific for the Raman reporter dyes Infrared 792 (IR-792) and Nile Blue (NB), respectively. Assay reactions containing dilutions of both target antigens yielded a reduction in the intensification of IR-792 and NB signature spectrum peaks and provided a conservative limit of detection of ~5 fg/ml for assays conducted in phosphate buffered saline buffer (PBS) and ~25 pg/ml for assays containing PBS spiked with fetal bovine serum. Based on the inherent simplicity of the assay, magnetic capture-based SERS assays afford promise as a biosensor platform that provides high-level multiplex detection sensitivity and can be adapted for portable diagnostic applications in limited resource settings.

1. Introduction

Sensitive and selective diagnostic assays are essential tools for the rapid identification of pathogenic agents and the implementation of prophylactic procedures for mitigating the spread of disease in human and animal populations. Current technologies are restricted, however, in the scope of their detection capabilities and fully integrated assay platforms have yet to be developed which are portable, user-friendly and cost-effective, and which also provide rapid, highly sensitive and discriminate multiplex test results (Posthuma-Trumpie et al., 2009; Maurer, 2011). In an effort to address these demands and thereby expand the repertoire of diagnostic testing capabilities, surface-enhanced Raman scattering (SERS) spectroscopy has emerged as a next generation biosensor technology which affords broad range bioanalyte detection (Porter et al., 2008; Bantz et al., 2011) and can be miniaturized for point-of-care (POC) applications (Lesaicherre et al., 2009; Carron and Cox, 2010).

Due to the weak inelastic light scattering properties of many clinically relevant bioanalytes, namely proteins and nucleic acids (Thomas and Agard, 1984), SERS-based assays developed for diagnostic applications are generally predicated on detection formats in which analyte capture positions a strong inelastic light scattering compound, or Raman reporter, in close proximity to aggregated noble metal nanoparticles (NP)s (i.e. Ag or Au) or roughened noble metal surfaces (Jeanmaire and van Duyne, 1977; Kerker, 1984). Upon laser excitation, the electromagnetic field enhancement arising from localized surface plasmon oscillations serves to magnify the vibrational and rotational Raman modes of the reporter compound (Zeman and Schatz, 1987), the recorded intensities of which provide a quantitative estimation of analyte detection levels. Based on these principles, SERS immunoassays developed for antigen-specific IgG detection have demonstrated a significant enhancement over the limit of detection (LOD) sensitivities provided by the ELISA (Neng et al., 2010), and LOD sensitivities in the range of 1–12 pg/ml have been reported for cancer biomarkers (Grubisha et al., 2003; Gong et al., 2007; Chon et al., 2009).

In addition to providing high level detection sensitivity, SERS affords several advantages over traditional immunoassay methodologies based on the use of fluorescent tags. These include the reduced susceptibility of Raman-active compounds to photobleaching (Braun et al., 2007), the large number of Raman compounds that are available as reporters for a wide range of laser excitation wavelengths (Sun et al., 2007), and most significantly, adaptability to high level multiplex applications. In contrast to the broad spectrum emissions of fluorescence, Raman spectra are characterized by

* Corresponding author. Tel.: +1 307 766 6524; fax: +1 307 766 6777.
E-mail address: pjohns27@uwyo.edu (P.A. Johnson).

0956-5663/$ - see front matter © 2012 Elsevier B.V. All rights reserved.
http://dx.doi.org/10.1016/j.bios.2012.08.048

narrow bandwidth peaks that confer distinct "signature" profiles (Graham et al., 2002; Porter et al., 2008). In efforts to develop multiplex assay platforms based on SERS, POC studies have demonstrated the sensitive detection and discrimination of clinically relevant DNA target sequences in hybridization creactions (Wang et al., 2009; Kang et al., 2010), as well as multiplex SERS imaging of intact cell surface receptors (Kennedy et al., 2010) and cell surface biomarkers specific for different cancers (Maiti et al., 2011). Additional studies have reported the application of SERS for detecting multiple food (Cam et al., 2010; Ravindranath et al., 2011) and water borne (Rule and Vikesland, 2009) bacterial pathogens in which intact cell capture was accomplished using SERS-active NPs conjugated with pathogen-specific antibodies.

In the present study, we describe a highly sensitive SERS-based immunoassay for the detection of multiple viral antigens. The antigens selected as target analytes, the West Nile virus (WNV) envelope (E) protein (Wang et al., 2001) and the Rift Valley Fever virus (RVFV) nucleocapsid N protein (Fafetine et al., 2007), are derived from zoonotic viruses which confer similar disease symptomologies in infected individuals (Kortekaas et al., 2010). The specific capture of both antigens in individual assay reactions was performed by incubation with mixtures of Au nanoparticles (GNPs) and paramagnetic nanoparticles (PMPs) conjugated with polyclonal antibodies (Pabs) specific for antigen recognition, and detection was provided by magnetic pull-down of the GNP/antigen/PMP immuno-recognition complexes and laser excitation of spectrally distinct Raman reporters bound to the GNPs. The LOD sensitivity we report here for the simultaneous detection of WNV E and RVFV N, ~5 fg/ml, is 200–2000-fold greater than the LOD sensitivities previously reported for single antigens using multi-step magnetic capture assays (Gong et al., 2007; Chon et al., 2009) and justifies a rational design approach for higher order multiplexing by simply adding GNP and PMP reagents specific for the recognition of each target analyte. In an effort to simulate realistic test conditions using biological specimens, assay reactions spiked with fetal bovine serum (FBS) yielded reduced LOD sensitivities, indicating the need to thoroughly evaluate the impact of interferents on assay performance and the implementation of modified assay procedures for mitigating these effects.

2. Experimental

2.1. Materials and chemicals

Bis-*N*-succinimidyl-(pentaethylene glycol) ester linker ($BS(PEG)_5$), Pierce™ protein A/G agarose and the Supersignal® West Pico Chemiluminescent Substrate kit were obtained from Thermo Scientific. Colloidal GNPs (60 nm, 2.6×10^{10} NPs/ml) were purchased from Ted Pella Inc. (Redding, CA) and Fe_3O_4 PMPs (~200 nm) were purchased from Nanostructured and Amorphous Materials, Inc. (Houston, TX). HiTrap™ NHS-activated HP columns were ordered from GE Healthcare (Piscataway, NJ) and all other chemicals used in the study were from Sigma-Aldrich. Chemical stock solutions were made using deionized water (18.2 MΩ cm^{-1}) filtered by passage through 0.2 μm Millipore syringe filtration units.

2.2. WNV E and RVFV N antigen/antibody reagents

The recombinant WNV E protein and rabbit anti-E Pabs used in this study have been previously described (Neng et al., 2010). Rabbit Pabs raised against recombinant RVFV N protein lacking the transmembrane domain were provided by Drolet et al. (2012). Prior to NP conjugation, non-specific anti-*E. coli* antibodies were removed from serum by adsorption to total *E. coli* protein-bound HiTrap™ columns, after which the sera were enriched for the IgG fraction by protein A/G affinity chromatography. To assess antibody/antigen specificity, replicate Western blots containing both antigens were probed individually with anti-E IgG and anti-N IgG, followed by incubation with HRP-conjugated goat anti-rabbit IgG and chemiluminescence detection.

2.3. Synthesis of silica-coated and antibody-bound PMPs

PMPs dispersed in anhydrous DMSO at a concentration of 1 mg/ml were silanized with amine-functional alkoxysilane by the addition of (3-aminopropyl) triethoxysilane (APTES) to a final concentration of 5% (v/v) (Cao et al., 2009). The mixture was shaken for 15 h at 40 °C, after which a magnet was applied for PMP collection and washings with DMSO to remove excess APTES. 2.5 mg of $BS(PEG)_5$ linker was then added to amine-functionalized PMPs resuspended in 1 ml of DMSO and the mixture was incubated for 6 h at room temperature. Following washes with phosphate buffered saline (PBS) pH 7.5 to remove excess linker and resuspension in 1 ml of PBS, 60 μl aliquots of the PMP/PEG conjugates were individually reacted with 10 μl of 6 mg/ml anti-E and anti-N IgG, and the mixtures were incubated for 6 h at room temperature with gentle shaking. Finally, the PMP bioconjugates, referred to hereafter as capture PMPs, were washed to remove unbound antibody and then resuspended in 120 μl PBS for use in assay reactions.

2.4. Synthesis of Raman reporter and antibody-bound GNPs

To normalize their SERS responses, the Raman reporter dyes Infrared-792 (IR-792) and Nile blue (NB) were adjusted to final concentrations of 0.3 μM and 40 μM, respectively, and then incubated for 1 h with 1 ml colloidal Au suspensions. The reporter-bound GNPs were then centrifuged at 10,000 *g* for 7 min to discard unbound reporter molecules, resuspended in 1 ml of PBS, and reacted with antibodies at the same concentration used for the synthesis of capture PMPs. For multiplex detection of both WNV E and RVFV N antigens, two sets of spectrally distinct reporter GNPs were made for specific recognition of each target antigen. Specifically, IR-792-coated GNPs were functionalized with anti-E IgG and the NB-coated GNPs were functionalized with anti-N IgG (Supplemental Fig. S1). Following incubation at room temperature for 2 h, the GNP bioconjugates were washed to remove unbound antibodies and then incubated for 1 h with 2% (w/v) bovine serum albumin (BSA) in PBS to ensure surface passivation and minimize non-specific interactions (Sheehan and Whitman, 2005; Giljohann et al., 2009). Finally, excess BSA was removed by centrifugation and reporter GNPs were resuspended in 1 ml of PBS for use in assay reactions.

2.5. Characterization of functionalized PMPs and reporter GNPs

Transmission electron microscopy (TEM) imaging of PMPs and GNPs deposited on carbon-coated mesh copper double grid films (Electron Microscopy Sciences, Hatfield, PA) was performed using a Hitachi-H7000 TEM (Hitachi Hi-Tech, Tokyo). Particle size distribution was determined by Dynamic Light Scattering (DLS) using a ZetaPALS spectrometer (Brookhaven Instruments, Holtsville, NY). The absorption spectrum of GNPs was measured using a SpectraMax® Plus^{384} spectrometer (Molecular Devices Inc., Sunnyvale, CA).

2.6. SERS detection of multiple antigen targets by magnetic capture

Multiplex assays were assembled by adding 50 μl of each reporter GNP preparation, 60 μl of PBS containing dilutions of WNV E and RVFV N antigen, and 20 μl of each capture PMP preparation. For serum interference experiments, final reaction volumes contained a range of FBS concentrations. Triplicate reactions for each concentration of antigen tested were incubated for 1 h at room temperature

and then quenched by the application of an external magnet, after which the concentrated pellet material was transferred to a glass slide for laser excitation using an ExamineR™ Raman microscope (DeltaNu, Laramie, WY) (120 mW power, 785 nm laser) equipped with NuSpec™ software for spectrum data acquisition and Nuimage™ mapping software. Spectroscopic analysis was conducted using Grams/AI™ software (Thermo Fischer Scientific). Raman spectra were recorded in the 200–2000 wave number range with the baseline off and are an average of 5 1 s data acquisitions.

3. Results and discussion

3.1. Multiplexed magnetic capture-based SERS detection scheme for viral antigens

The essential features of the immunoassay developed for magnetic capture and SERS detection of target antigen are illustrated in Fig. 1. Reporter GNPs and capture PMPs are first incubated with antigen, after which extraction of developed GNP/antigen/PMP immuno-recognition complexes from the solution matrix by the application of an external magnet source serves to concentrate Raman reporter dyes within the focus beam of the interrogating laser. As a consequence of magnetic pull-down, the surface-adsorbed reporters are also favorably positioned within the collective enhanced electromagnetic fields, or "hot spots", of aggregated SERS substrates (Michaels et al., 2000; Le Ru et al., 2008). For multiplex detection of WNV E and RVFV N antigen, immunoassay reactions include an assembly of capture PMPs and spectrally distinct reporter GNPs that specifically recognize each target antigen. Detection sensitivity is determined by the avidity of antigen/antibody binding interactions and the effective concentration of each Raman reporter dye in the magnetically concentrated reaction pellet, and selectivity is dependent on the resolution of peaks corresponding to each reporter in mixed spectra.

3.2. Synthesis and characterization of reporter GNPs and capture PMPs

To normalize the SERS response of reporter GNPs for multiplexing, varying concentrations of IR-792 and NB were adsorbed to colloidal Au preparations and laser-excited spectra were then evaluated for the relative peak intensification of washed particles. Using this procedure, 40 μM NB and 0.3 μM IR-792 were found to provide comparable enhancements for the 591 cm^{-1} peak of NB and the 524 and 556 cm^{-1} peaks of IR-792 (Supplemental Fig. S1). The higher concentration required for NB is attributed to its weaker Raman cross-section (von Maltzahn et al., 2009), and may also result from a higher dissociation constant with Au surfaces as well.

UV–vis spectra taken at successive steps in the synthesis of reporter GNPs demonstrated a progressive shift in the position of the surface plasmon peak to longer wavelengths. As shown for the fabrication of reporter GNPs for WNV E detection (Fig. 2), the extinction maximum of 530 nm, which is characteristic of 60 nm GNPs (Creighton, 1982), shifted to 538 nm upon the addition of IR-792 and then to 540 nm following incubation with anti-E IgG. Red shifting of the extinction maximum is a common optical property of GNPs following surface immobilization and is dependent upon several variables, which can include particle size, shape, polarizability, the extent of aggregation versus dispersion, and the refractive index of the medium (Link and El-Sayed, 1999; Zeng et al., 2011). Although the peak broadening we observed can be an indicator of GNP aggregation (Porter et al. 2008), TEM imaging indicated a high level of particle dispersion and only minor aggregate formation (Supplemental Fig. S2).

DLS measurements of reporter GNPs and capture MNPs provided additional supportive evidence for particle dispersion and showed increases in average particle size which correlated with surface modifications. The functionalization of 60 nm GNPs with IR-792 and anti-E IgG, for instance, yielded particles with an average diameter of 77.3 ± 15.5 nm. Likewise, 200 nm core PMPs increased in average diameter to 209.2 ± 22.7 nm following silica encapsulation and conjugation with anti-E IgG. Although reporter GNPs are often synthesized with an outer silica shell to prevent the passive loss of adsorbed reporter molecules, as well as to promote particle dispersion and reduce non-specific binding interactions (Sha et al., 2008; Huang et al., 2011), we have found that surface modification by non-covalent interactions with Raman reporters and proteins is suitable for POC assays. This eliminates the number of steps required for surface functionalization and yields particles that are dispersed and fully stable over the course of the experiments (Qu et al., 2012; Chen et al., 2012).

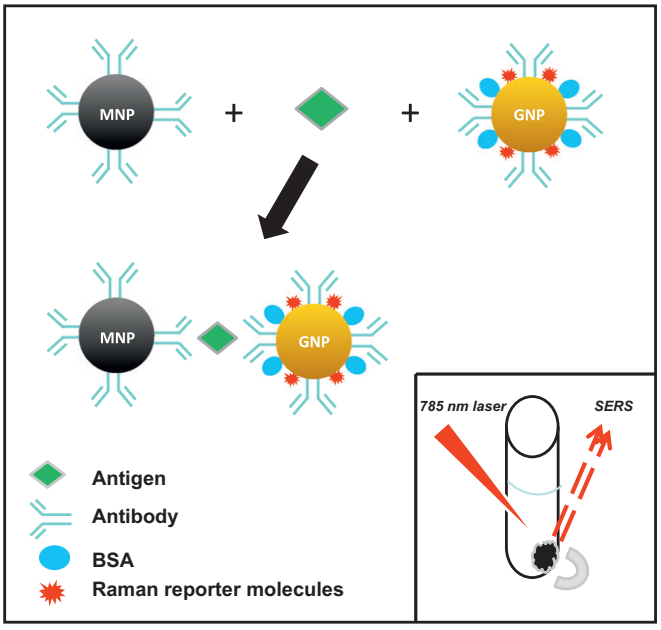

Fig. 1. Magnetic capture and SERS detection of viral antigens.

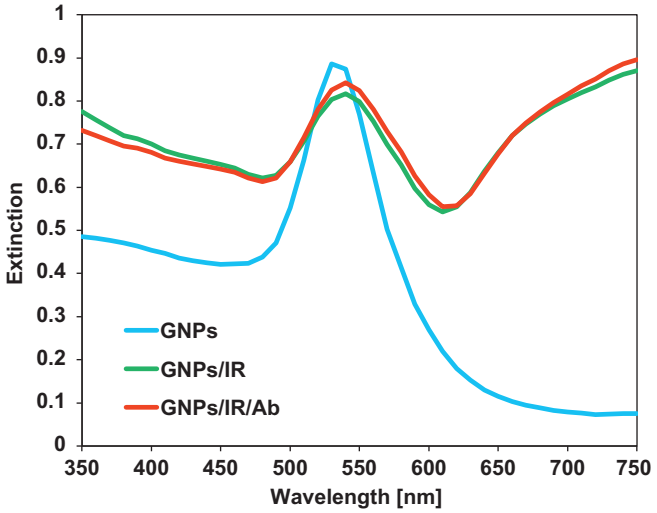

Fig. 2. UV–vis absorption spectra of GNPs (blue scan, 530 nm), IR-792-adsorbed GNPs (green scan, 538 nm) and IR-792-adsorbed GNPs conjugated with anti-E IgG (red scan, 540 nm). (For interpretation of the references to color in this figure legend, the reader is referred to the web version of this article.)

3.3. Assembly of reagents for immunoassay development

Multiplexed immunoassays for the range of WNV E and RVFV N antigen concentrations tested were conducted using $\sim 1.2-1.3\times 10^9$ reporter GNPs and capture PMPs. The particle number estimate for reporter GNPs was provided by the vendor and concentrations yielding an equivalent number of capture PMPs were determined using the density of bulk Fe_3O_4 (5.15 g/cm^3). These conditions provide a rational approach to multiplex reagent assembly, but the optimal stoichiometric ratio of reporter GNPs and capture PMPs for providing maximum detection sensitivity has not been empirically determined.

Other factors likely to impact assay performance are the quality of antibody reagents and their surface coverage levels. While Western blotting revealed high binding avidities and the absence of cross-reactivity for our antigen/antibody reagents, we were unable to obtain quantitative estimates for levels of GNP and PMP-bound IgGs. These are difficult measurements to obtain, as methods for protein determination (e.g. 260 nm absorbance, dye binding assays) rely on measurements of absorbance maxima that overlap with the UV–vis absorbance spectra of GNPs (Lyon et al., 2004) and PMPs (Tang et al., 2003). Also, we have found that the method of inferring surface coverage levels by monitoring the level of unbound protein (Liu and Wong, 2009) provides measurements with high levels of statistical error.

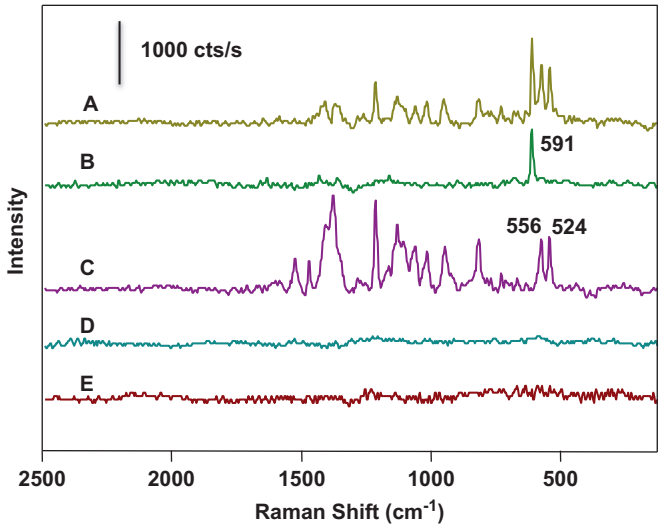

Fig. 3. Magnetic capture-based SERS detection of WNV E and RVFV N antigens. Immunoassay reactions containing GNPs and PMPs for multiplex detection of WNV E and RVFV N (spectrum A), GNPs and PMPs for detection of RVFV N (spectrum B), GNPs and PMPs for detection of WNV E (spectrum C), GNPs and PMPs for RVFV N recognition and WNV E antigen (spectrum D), and GNPs and PMPs for WNV E recognition and RVFV N antigen. All reactions contained 5 pg/ml of antigen and spectra were baseline corrected.

3.4. Multiplexed SERS detection of magnetically captured WNV E and RVFV N antigens

Multiplex assay reactions incubated for 1 h and then magnetically concentrated for laser excitation yielded spectra that were a mixture of the individual Raman spectra for NB and IR-792. As shown in Fig. 3, spectra for assays containing 5 pg/ml of each antigen were characterized by a nested triplet of dominant peaks at 591 cm^{-1}, 556 cm^{-1} and 524^{-1} (spectrum A), the 591 cm^{-1} peak of which is diagnostic for NB excitation and RVFV N capture (spectrum B) and the 556 cm^{-1} and 524 cm^{-1} peaks which are indicators of IR-792 excitation and WNV E capture (spectrum C). Control reactions demonstrating detection specificity are shown by the absence of SERS signaling in single antigen capture assays in which reporter GNPs and capture PMPs functionalized for the detection of either WNV E (spectrum D) or RVFV N (spectrum E) were incubated with the other antigen. Negative control reactions in which antigen were omitted from reagents assembled for multiplex detection (spectrum F) yielded background spectra identical to spectra D and E (data not shown).

The LOD sensitivity was determined by acquiring spectra for assay reactions containing a 10-fold serial dilution series of both antigens and identifying the lowest concentration at which the 591 cm^{-1}, 556 cm^{-1}and 524 cm^{-1} peaks could still be detected. As shown for antigen concentrations in the range of 50–0.005 pg/ml (Fig. 4A), the acquired spectra demonstrated a progressive reduction in overall peak intensification and provide a conservative LOD of $\sim$5 fg/ml (spectrum E). Whereas the relative intensifications of the 591 cm^{-1}, 556 cm^{-1} and 524 cm^{-1} peaks correlated well with antigen concentration. We have found, however, that this is not the case for peaks in the 800–1600 cm^{-1} range of the vibrational spectrum for IR-792. Peak height and signal-to-noise measurements

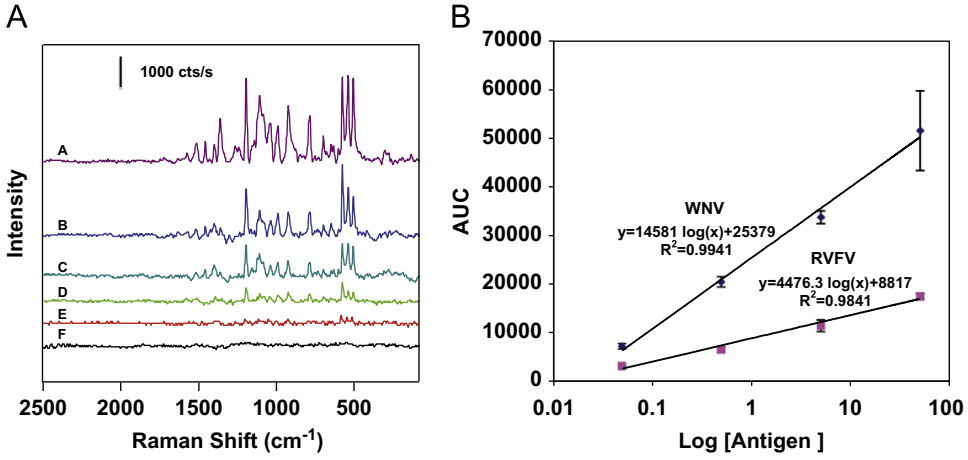

Fig. 4. (A) SERS spectra for multiplex immunoassays containing serial dilutions of WNV E and RVFV N antigen. The top 5 spectra correspond to antigen concentrations of 50 pg/ml (spectrum A), 5 pg/ml (spectrum B), 0.5 pg/ml (spectrum C), 0.05 pg/ml (spectrum D) and 0.005 pg/ml (spectrum E). The bottom spectrum is for an assay reaction lacking both antigens (spectrum F). (B) Plot of the $\log_{10}$ concentration of antigen versus the relative signal intensification (area under curve, AUC) of the 524 and 556 cm^{-1} peaks diagnostic for WNV E antigen detection and the 591 cm^{-1} peak diagnostic for RVFV N antigen detection. Error bars indicate the standard deviation for 3 replicate measurements at each dilution tested. Each measurement is the average of 5 1s spectral acquisitions.

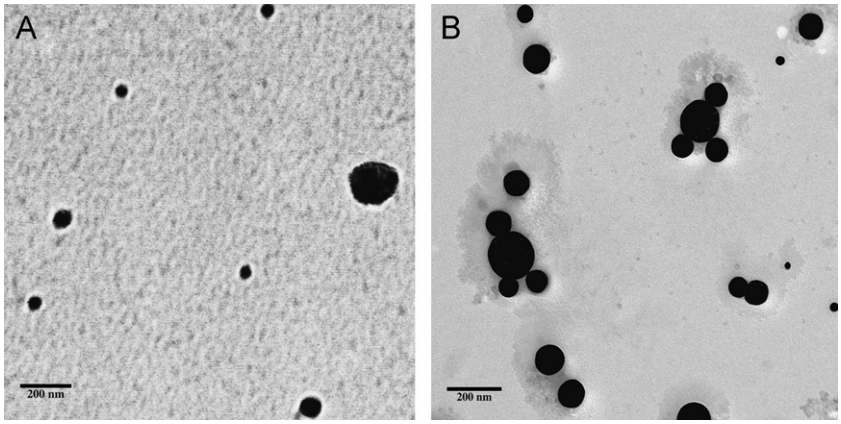

Fig. 5. TEM image of GNPs and PMPs in the presence of WNV E antigen.

in this region of the spectrum are prone to fluctuations that do not track changes in antigen concentration.

To determine the quantitative response of SERS signaling intensification to antigen capture, multiplex spectra were background corrected and the relative areas of the NB 591 cm^{-1} peak and the IR-792 556 and 524 cm^{-1} peaks were independently plotted as a function of their respective antigen concentrations. A log-linear relationship for over 3 orders of magnitude was found (Fig. 4B) and linear regression analysis yielded an R^2 value of 0.9941 for WNV E detection and an R^2 of 0.9841 for RVFV N detection. The variability shown for E antigen detection at the highest concentration tested was due to technical difficulties associated with baseline correction for fluorescence interference.

Physical evidence supportive of the mechanism for antigen capture and subsequent laser interrogation is provided in TEM images showing the antigen-dependent association of reporter GNPs and capture PMPs. Whereas assay mixtures of reporter GNPs and capture PMPs indicate particle dispersion in the absence of antigen (Supplementary Fig. S2), a TEM image of assay mixtures containing antigen shows 2 GNP/antigen/PMP complexes, each of which consists of a single PMP and 3 surface-associated GNPs (Fig. 5).

3.5. Effect of FBS on multiplex detection sensitivity

To evaluate assay performance using a simulant of serum, multiplex assays were conducted in PBS spiked with FBS. Initial experimentation using WNV E and RVFV N antigen concentrations in the pg/ml range and FBS concentrations $>40\%$ (w/v) yielded weak, or undetectable SERS responses, indicating a strong interference effect by FBS (data not shown). Reduction of the FBS concentration to 5% (w/v) in assays containing antigens in the ng/ml concentration range, however, yielded intense spectra that served as a baseline for determining LOD sensitivity. As shown in Fig. 6, assays containing 100–0.1 ng/ml of each antigen (spectra A–D) provided a reduction in signaling intensification as the concentration was decreased and a LOD sensitivity 0.1 ng/ml (spectrum D). Although the $\log_{10}$[antigen] demonstrates a linear relationship with calculated diagnostic peak area (WNV E, $R^2=0.9724$; RVFV N, $R^2=0.9896$), the measured LOD is $\sim$20,000-fold lower than the LOD recorded for assays conducted in PBS buffer.

In light of our finding that non-specific, inter-particle interactions do not develop in the presence of FBS (Fig. 6, spectrum E), it is probable that the dramatic reduction in LOD sensitivity is due to FBS interference with the antigen-mediated tethering of GNPs and PMPs. The mechanism by which this occurs, however, is unclear. In an effort to evaluate the suppressive effect of FBS with regard to SERS immunoassays that have reported antigen detection in human clinical samples, we find that significant

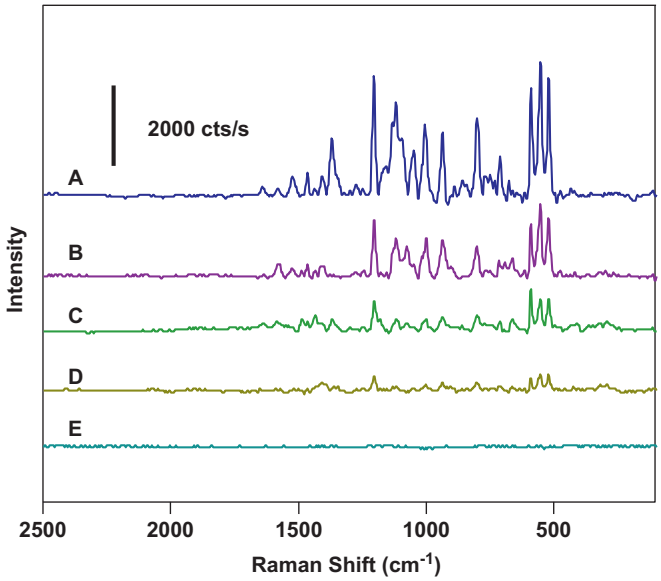

Fig. 6. SERS spectra for multiplex immunoassays containing 5% FBS and serial dilutions of WNV E and RVFV N antigen. The Top 4 spectra correspond to antigen concentrations of 100 ng/ml (spectrum A), 10 ng/ml (spectrum B), 1 ng/ml (spectrum C), 0.1 ng/ml (spectrum D). The bottom spectrum is for an assay reaction lacking both antigens (spectrum E).

differences in assay design and test procedures preclude valid comparisons. In a seminal study reported by Sha et al. (2008), for instance, the detection of epithelial tumor cells in whole blood using antibody-functionalized GNPs and PMPs was reported on the basis of cells/ml. Interestingly, however, the recent detection of a marker for pancreatic cancer (i.e. MUC4) in human serum employed a SERS-based immunoassay and 1:20 dilutions of pooled patient sera as test samples (Wang et al., 2011). This concurs with the highest FBS concentration we determined to be permissible for sensitive WNV E and RVFV N detection.

4. Conclusion

Due to the inherent advantages of SERS as an analytical tool for facilitating high-level multiplex capabilities, a significant research impetus has emerged which is focused on the development and implementation of this technology for improved diagnostic testing. In this study, we have described a magnetic capture-based SERS assay for the simultaneous detection of unrelated viral coat and capsid antigens that provides an exceptionally sensitive LOD.

Although other SERS assays have been reported which incorporate magnetic capture as an integral component of the detection platform, single antigen detection is invariably reported. In the only other study of which we are aware in which the simultaneous detection of 2 antigens has been demonstrated, the assay procedure required several processing steps and the LOD measured for each antigen was in the range of 1–2 ng/ml (Chon et al., 2011). Rather than attributing this discrepancy to differences in experimental design or procedures for the synthesis of assay reagents, we are of the opinion that the use of antigen/antibody reagents prepared in-house and thoroughly assessed for their avidities is a crucial determinant of assay performance. Despite the ease with which commercially prepared immunologicals can be adopted for assay development, high-throughput procedures are by necessity implemented during the production process and quality control measures are often lacking.

Aside from establishing incremental improvements in model assay development, however, significant technical obstacles remain that will need to be overcome before the assay platform outlined here, or other SERS immunoassays that have been developed for that matter, can be adapted for high-level multiplexing and overall robust assay performance. These include the development of instrumentation with laser optics that minimize Raman reporter fluorescence emissions, the identification of a suite of several spectrally distinct Raman reporters that are defined by peak intensifications that reliably correlate with antigen concentration, and the development of procedures for reagent synthesis that are optimized for reproducible antigen capture and detection. Also, as suggested here by assay reactions conducted in the presence of FBS, the testing of clinical specimens will require optimized procedures for both sample preparation and the minimization of the inhibitory effects of molecules and compounds present in different specimens. Currently, we are addressing these and other experimental variables that will need to be optimized for the goal of developing an assay platform consisting of consumable reagents for multiplexed immunoassay detection and a portable Raman reader that is engineered for the magnetic capture of assay reactions.

Acknowledgments

The authors wish to acknowledge the financial support of the Kansas Bioscience Authority (KBA) (Olathe, KS). We also thank the ABADRU unit of CGAHR (ARS/USDA, Manhattan, KS) for providing recombinant RVFV N antigen and rabbit anti-N Pabs. The contents of this publication are the responsibility of the authors and do not necessarily represent the views of the KBA or the USDA.

Appendix A. Supporting information

Supplementary data associated with this article can be found in the online version at http://dx.doi.org/10.1016/j.bios.2012.08.048.

References

Bantz, K.C., Meyer, A.F., Wittenberg, N.J., Im, H., Kurtulus, O., Lee, S.H., Lindquist, N.C., Oh, S.H., Haynes, C.L., 2011. Physical Chemistry Chemical Physics 24, 11551–11567.
Braun, G., Lee, S.J., Dante, M., Nguyen, T.Q., Moskovits, M., Reich, N., 2007. Journal of the American Chemical Society 129, 6378–6379.
Cam, D., Keseroglu, K., Kahraman, M., Sahin, F., Culha, M., 2010. Journal of Raman Spectroscopy 41, 484–489.
Cao, H., He, J., Deng, L., Gao, X., 2009. Applied Surface Science 255, 7974–7980.
Carron, K., Cox, R., 2010. Analytical Chemistry 82, 3419–3425.
Chen, L., Han, X.X., Guo, Z., Wang, X., Ruan, W., Song, W., Zhao, B., Ozaki, Y., 2012. Analytical Methods 4, 1643–1647.
Chon, H., Lee, S., Son, S.W., Oh, C.H., Choo, J., 2009. Analytical Chemistry 81, 3029–3034.
Chon, H., Lee, S.-Y., Yoon, S.-Y., Chang, S.-I., Lim, D.W., Choo, J., 2011. Chemical Communications 47, 12515–12517.
Creighton, J.A., 1982. In: Chang, R.K., Furtek, T.E. (Eds.), Surface-Enhanced Raman Scattering. Plenum Press, New York, pp. 315–337.
Drolet, B.S., Weingartl, H.M., Jiang, J., Neufeld, J., Marszal, P., Lindsay, R., Miller, M.M., Czub, M., Wilson, W.C., 2012. Journal of Virological Methods 179, 373–382.
Fafetine, J.M., Tijhaar, E., Paweska, J.T., Neves, L.C., Hendriks, J., Swanepoel, R., Coetzer, J.A., Egberink, H.F., Rutten, V.P., 2007. Veterinary Microbiology 121, 29–38.
Giljohann, D.A., Seferos, D.S., Prigodich, A.E., Patel, P.C., Mirkin, C.A., 2009. Journal of the American Chemical Society 131, 2072–2073.
Gong, J.-L., Liang, Y., Chen, J.-W., Jiang, J.-H., Shen, G.-L., Yu, R.-Q., 2007. Biosensors & Bioelectronics 22, 1501–1507.
Graham, D., Mallinder, B.J., Whitcombe, D., Watson, N.D., Smith, W.E., 2002. Analytical Chemistry 74, 1069–1074.
Grubisha, D.S., Lipert, R.J., Park, H.-Y., Driskell, J., Porter, M.D., 2003. Analytical Chemistry 75, 5936–5943.
Huang, J., Kim, K.H., Choi, N., Chon, H., Lee, S., Choo, J., 2011. Langmuir: The ACS journal of Surfaces and Colloids 201, 10228–10233.
Jeanmaire, D.L., van Duyne, R.P., 1977. Journal of Electroanalytical Chemistry 84, 1–20.
Kang, T., Yoo, S.M., Yoon, I., Lee, S.Y., Kim, B., 2010. Nano Letters 10, 1189–1193.
Kennedy, D.C., Hoop, K.A., Tay, L.-L., Pezacki, J.P., 2010. Nanoscale 2, 1413–1416.
Kerker, M., 1984. Accounts of Chemical Research 17, 271–277.
Kortekaas, J., Ergonul, O., Moorman, R.J., 2010. Vector Borne and Zoonotic Diseases (Larchmont, NY) 10, 709–718.
Le Ru, E.C., Meyer, M., Blackie, E., Etchegoin, P.G., 2008. Journal of Raman Spectroscopy 39, 127–134.
Lesaicherre, M.L., Paxon, T.L., Mondello, F.J., Burrell, M.C., Linsebigler, A., 2009. Proceedings of the SPIE 7319 (73190C), 1–11.
Link, S., El-Sayed, M.A., 1999. The journal of Physical Chemistry B 103, 4212–4217.
Liu, X., Wong, D.K.Y., 2009. Talanta 77, 1437–1443.
Lyon, J.L., Fleming, D.A., Stone, M.B., Schiffer, P., Williams, M.E., 2004. Nano Letters 4, 719–724.
Maiti, K.K., Samanta, A., Vendrell, M., Soh, K.-S., Olivo, M., Chang, Y.-T., 2011. Chemical Communications 47, 3514–3516.
Maurer, J.J., 2011. Annual Review of Food Science and Technology 2, 259–279.
Michaels, A.M., Jiang, J., Brus, L., 2000. The Journal of Physical Chemistry B 104, 11965–11971.
Neng, J., Harpster, M.H., Zhang, H., Mecham, J.O., Wilson, W.C., Johnson, P.A., 2010. Biosensors and Bioelectronics 26, 1009–1015.
Porter, M.D., Lipert, R.J., Siperko, L.M., Wang, G., Narayanan, R., 2008. Chemical Society Reviews 37, 1001–1011.
Posthuma-Trumpie, G.A., Korf, J., von Amerongen, A., 2009. Analytical and Bioanalytical Chemistry 393, 569–582.
Qu, L.-L., Li, D.-W., Xue, J.-Q., Zhai, W.-L., Fossey, J.-S., Long, Y.-T., 2012. Lab on a Chip 12, 876–881.
Ravindranath, S.P., Wang, Y., Irudayaraj, J., 2011. Sensors and Actuators B 152, 183–190.
Rule, K.L., Vikesland, P.J., 2009. Environmental Science and Technology 43, 1147–1152.
Sha, M.Y., Xu, H., Natan, M.J., Cromer, R., 2008. Journal of the American Chemical Society 130, 17214–17215.
Sheehan, P.E., Whitman, L.J., 2005. Nano Letters 5, 803–807.
Sun, L., Yu., C., Irudayaraj, J., 2007. Analytical Chemistry 79, 3981–3988.
Tang, J., Myers, M., Bosnick, K.A., Brus, L.E., 2003. The Journal of Physical Chemistry B 107, 7501–7506.
Thomas Jr., G.J., Agard, D.A., 1984. Biophysical Journal 46, 763–768.
von Maltzahn, G., Centrone, A., Park, J.-H., Ramanathan, R., Sailor, M.J., Hatton, T.A., Bhatia, S.N., 2009. Advanced Materials (Weinheim, Germany) 21, 3175–3180.
Wang, T., Anderson, J.F., Anal. Magnarelli, L.A., Bushmich, S., Wong, S., Koski, R.A., Fikrig, E., 2001. Annals of the New York Academy of Sciences 951, 325–327.
Wang, G., Lipert, R.J., Jain, M., Kaur, S., Chakraboty, S., Torres, M.P., Batra, S.K., Brand, R.E., Porter, M.D., 2011. Analytical Chemistry 83, 2554–2561.
Zeman, E.J., Schatz, G.C., 1987. The Journal of Physical Chemistry 91, 634–643.
Zeng, S., Yong, K.-T., Roy, I., Dinh, X._.Q., Yu, X., Luan, F., 2011. Plasmonics 6, 491–506.